(Received 22 May 2024, Accepted 25 June 2024, Scheduled 16 July 2024)

Dual-Band Circularly Polarized Antenna with Wide Axial-Ratio and Gain Beamwidths for High-Precision BDS Applications

Junhao Ren, Hongmei Liu*, Youjie Zeng, Zhongbao Wang, and Shaojun Fang

School of Information Science and Technology, Dalian Maritime University, Dalian 116026, Liaoning, China

ABSTRACT: In this paper, a dual-band circularly polarized (CP) antenna with wide axial ratio and gain beamwidths is proposed for high-precision BDS applications. The radiator consists of four groups of dipoles, eight metal columns, and a reflector. The half-power beamwidth (HPBW) can be effectively increased by bending a portion of the dipole into an arc and loading a series of metal columns on the ground. Besides, a reactive impedance structure (RIS) is inserted and serves as a reflector to improve the axial ratio beamwidth (ARBW) and obtain unidirectional radiation. At the same layer of the dipoles, a four-feed network is presented to provide stable quadrature-phase excitation. For validation, the designed antenna is manufactured, where the overall size is $0.48\lambda \times 0.48\lambda \times 0.12\lambda$. Measurement results suggest that the proposed antenna is capable of operating efficiently within the frequency range of 1.17–1.22 GHz (4.2%) and 1.5–1.65 GHz (9.5%), which covers BDS B1 and B2 bands. Moreover, at four main planes, the measured 3-dB ARBW/HPBW are more than 121°/121° and 150°/198° at 1.207 GHz and 1.561 GHz, respectively. Considering that the proposed CP antenna exhibits wide overlapped beamwidth and small size, it is conducive to high-precision positioning in BDS applications.

1. INTRODUCTION

Beidou navigation system (BDS) has been employed extensively in commercial, military, and civil fields, where the circularly polarized (CP) antenna is its critical component [1–4]. In order to receive stable signals both at low and high altitudes for high-precision positioning, the CP antenna needs to have a wide beamwidth, which includes wide 3-dB ARBW and wide HPBW. In recent studies, some ideas for enhancing the 3-dB ARBW [5–14] and HPBW [15–18] of CP antennas have been proposed. Nevertheless few of researches have improved both.

In [19], by arranging two perpendicular bowed patch dipole pairs that are in alignment with the hemispherical surface, it is possible to improve the HPBW and 3-dB ARBW to 111° and 196°, respectively. In [20], the introduction of four parasitic elements, each of which consists of a perpendicular metallic plate and a flat triangle patch, has resulted in a progress of both the 3-dB ARBW and HPBW to over 110°. In [21], the loading of a metal strip on a quadrifilar helix antenna enables the realization of 3-dB ARBWs of more than 163° and HPBWs of more than 120° in two frequencies. It is demonstrated that unevenly compressed dipoles that operate in high-order mode [22] can effectively widen the 3-dB ARBWs and HPBWs of an antenna to be larger than 118° and 109°, respectively. Then, the dielectric lens as a cover [23] is presented to enlarge the HPBW from 69° to 170°, whilst maintaining 3-dB ARBWs of over 200°. Nevertheless, the structure is accompanied by the disadvantages including considerable weight and size. In [24], it can be observed that the HPBWs and 3-dB ARBWs are enhanced to 147° and 180°, respectively, by introducing parasitic strips and reflectors while the dimensions remain considerable. Moreover, the majority of these researches concentrate on the wide beamwidth of main cut planes (such as $\varphi = 0°$ and $\varphi = 90°$ planes), which cannot provide an accurate representation of the antenna's overall radiation performance. In order to assess the CP radiation performance, it is necessary to observe at least four distinct cut planes. Although in our previous work [25] by introducing vertical current and reactive impedance structure (RIS), the HPBWs and 3-dB ARBWs in four main cut planes are enhanced to be larger than 131° and 135°, respectively, it is limited to single-band operation.

In this paper, a dual-band CP antenna with wide HPBW and 3-dB ARBW is introduced for BDS application. It has the merits of: (1) wide overlapped 3-dB ARBW and HPBW at dual bands, (2) wide AR bandwidth, (3) uniform CP radiation, (4) small size. For validation, a prototype with a total size of $0.48\lambda \times 0.48\lambda \times 0.12\lambda$ is fabricated. The results of the measurement indicate that the presented antenna can operate within frequency ranges of 1.17–1.22 GHz and 1.5–1.65 GHz, which cover the BDS B1 and B2 bands. Moreover, the overlapped beamwidths at 1.207 GHz and 1.561 GHz are more than 121° and 150°, respectively.

2. ANTENNA CONFIGURATION

Figure 1 shows the structure of the presented dual-band CP antenna that consists of four groups of dipoles, eight metal columns, a reflector, and a quadrature four-feed network. Four groups of dipoles are printed on an F4B substrate (named as substrate I, $\varepsilon_r = 3.5$, $\tan\delta = 0.003$, $h_1 = 1.5$ mm). Each group is composed of two groups of radiation arms, which are connected by arc-shaped metal strips. It should be noted that the

* Corresponding author: Hongmei Liu (lhm323@ dlmu.edu.cn).

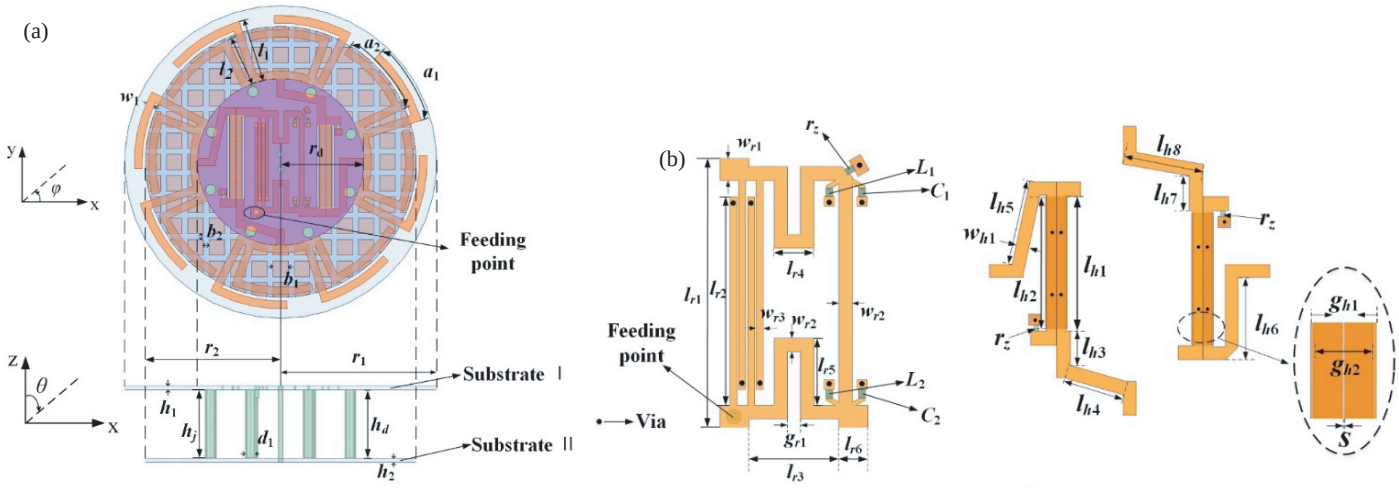

FIGURE 1. Structure of the proposed CP antenna. (a) Antenna. (b) Feeding network. ($l_1 = 24.5$ mm, $l_2 = 19.2$ mm, $w_1 = 3$ mm, $a_1 = 31$ deg, $a_2 = 36$ deg, $r_1 = 60$ mm, $r_2 = 52$ mm, $r_d = 32$ mm, $h_1 = 1.5$ mm, $h_2 = 1.5$ mm, $h_d = 27.3$ mm, $h_j = 27$ mm, $d_1 = 4$ mm, $b_1 = 6$ mm, $b_2 = 2.2$ mm, $l_{r1} = 41.8$ mm, $l_{r2} = 32.5$ mm, $l_{r3} = 14$ mm, $l_{r4} = 6.2$ mm, $l_{r5} = 10.5$ mm, $l_{r6} = 4.5$ mm, $w_{r1} = 3$ mm, $w_{r2} = 2.1$ mm, $w_{r3} = 1.1$ mm, $g_{r1} = 2$ mm, $l_{h1} = 31.6$ mm, $l_{h2} = 31$ mm, $l_{h3} = 8.1$ mm, $l_{h4} = 14.4$ mm, $l_{h5} = 20.1$ mm, $l_{h6} = 19.4$ mm, $l_{h7} = 8.2$ mm, $l_{h8} = 18.5$ mm, $w_{h1} = 3$ mm, $g_{h1} = 5.1$ mm, $g_{h2} = 4.5$ mm, $s = 0.1$ mm, $r_z = 50\,\Omega$, $L_1 = 15$ nH, $L_2 = 18$ nH, $C_1 = 0.5$ pF, $C_2 = 0.5$ pF).

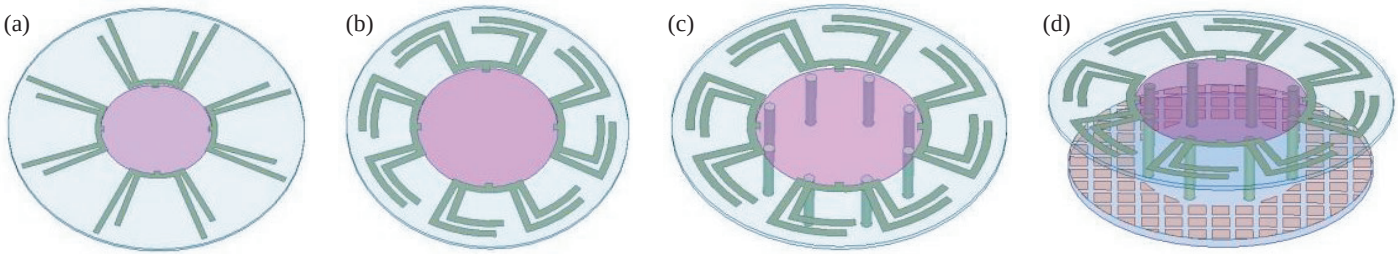

FIGURE 2. Evolutions of the proposed CP antenna. (a) Ant. 1. (b) Ant. 2. (c) Ant. 3. (d) Ant. 4.

radiation arm includes an inner metal strip and an outer metal strip. The mentioned outer metal strip is divided into a straight arm and a curved arm. The length of the straight arm is l_1, and the curved arm is an arc with an angle of a_1, where the center is the same an the center of substrate I. Similarly, the straight arm for the inner metal strip has a length of l_2, and the curved arm has an angle of a_2. The angle gap between radiation arms in each group is 45°. The width of all metallic strips is designed as w_1.

Here, the RIS is set as the reflector to obtain small size and achieve unilateral radiation concurrently. It is positioned below substrate I at a distance of h_d and printed on an FR4 substrate (named as substrate II, $\varepsilon_r = 4.4$, $\tan\delta = 0.003$, $h_2 = 1.5$ mm). The radius of substrate II is r_2. It is covered by some uniformly arranged square patches except for the circular surface with the radius of r_d. Each patch's length is designed as b_1, and the distance between two patches is denoted as b_2. The ground-based attachment of eight metal columns serves the purpose of expanding the HPBW. The diameter and length of the metal column are denoted by d_1 and h_j, respectively.

In order to achieve the generation of equivalent amplitude signals with sequentially orthogonal phases, it is proposed that a orthogonal four-feed network should be designed, which is composed of two 90° directional couplers and a rat-race coupler. In addition, meander lines are utilized to achieve small size and better integration with antennas. The configuration of the network is given in Fig. 1(b). It is observed that the rat-race coupler and the two couplers are etched on the upper surface of substrate I. To achieve flat output amplitude and phase performances in dual bands, the rat-race coupler in [26] is adopted which owns the feature of flat output distributions. Besides, parallel coupled lines are used to form the 90° directional couplers. Since tight coupling of 3 dB is hard to implement by using the single-layer coupled lines, enhanced coupling structure [27] is utilized.

3. DESIGN EVOLUTIONS AND PARAMETRIC STUDY

3.1. Design Evolutions

In this section, design evolutions of the proposed antenna are introduced, and performance comparisons are provided for understanding the functions of each section in Fig. 3. However, the comparisons are conducted on the basis of the optimized axial ratio and return loss.

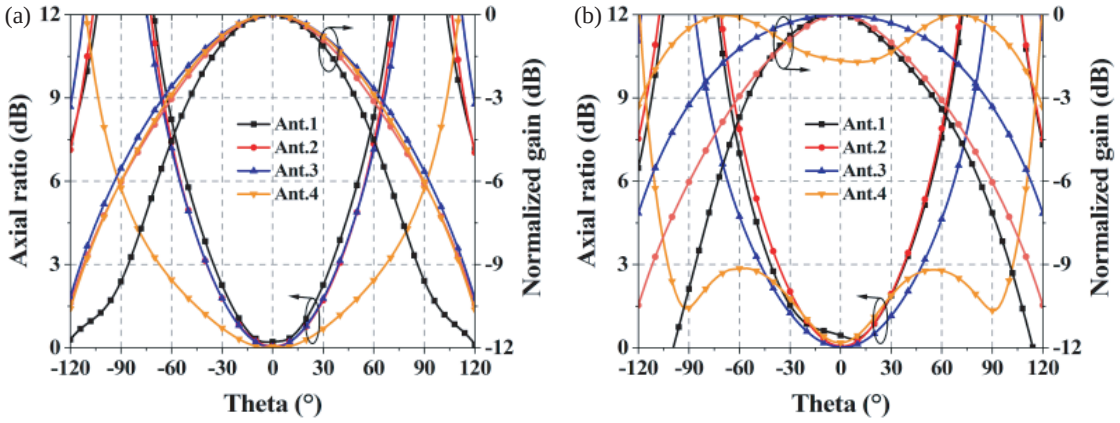

FIGURE 3. Performances comparisons among different evolutions. (a) ARBWs and HPBWs at 1.207 GHz (b) ARBWs and HPBWs at 1.561 GHz.

The initial structure (Ant. 1) is shown in Fig. 2(a), which consists of four groups of dipoles. To achieve dual-band operation, each dipole owns a long arm and a short arm. In addition, the four groups of dipoles are arranged with an angle gap of 45°, which results in uniform angular radiation. By tuning the length of the dipoles, Ant. 1 can operate at the center frequencies of 1.207 GHz and 1.561 GHz. As shown in Fig. 3, the simulated 3-dB ARBW/HPBW of Ant. 1 are 68°/98° and 76°/110° at two frequencies, respectively.

To enlarge the HPBW, part of the dipole is bent into an arc (Ant. 2), as shown in Fig. 2(b). It also benefits for size reduction. Compared with Ant. 1, the HPBW is enlarged by about 18° and 10° at the two frequencies. Then, eight metal columns are loaded to the ground (Ant. 3) under the theory that vertical current as the monopole has the ability to enhance the HPBW through far-field superposition. It can be demonstrated in Fig. 3 that the HPBWs are significantly enlarged to 130° and 170° at the two frequencies. One drawback is that these methods have less influence on the 3-dB ARBW.

Finally, to achieve comparable 3-dB ARBW with HPBW, the RIS is introduced below the antenna, which also serves as a reflector to obtain unidirectional radiation. The location and size of the RIS can be adjusted in order to alter the phase difference of the reflection phase, which consequently affects the phase and amplitude of the two linearly polarized modes of the CP antenna, with the objective of expanding the 3-dB ARBW. Fig. 4 gives the reflection phase for the RIS unit cell. It is noted that in this design the RIS is not only used for obtaining unidirectional radiation, but also benefits for beamwidth improvement. Since both of the goals are based on the reflection phase of the RIS, which belongs to the mechanism of far-field superposition, a tradeoff is made between the two goals. It can be seen in Fig. 3 that the 3-dB ARBW is improved to 134° and 204° at the two frequencies. While the HPBW remains essentially unchanged at 1.207 GHz, a slight decrease to 124° has been observed. At 1.561 GHz, the HPBW is enlarged to 230°.

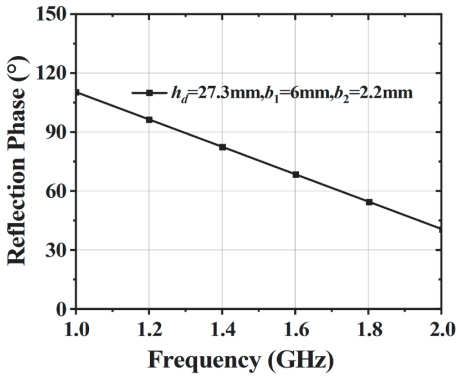

FIGURE 4. Reflection phase for the RIS unit cell.

3.2. Parametric Study

It is noted that the HPBWs and 3-dB ARBWs are influenced by the RIS and metal column during simulation. Following the studies, it is determined that the location of the RIS (h_d) and the length of the metal columns (h_j) have main effects. The impact of these variables on performance will be shown in this section.

Figures 5 and 6 illustrate the simulated normalized gain and the 3-dB ARBWs for varied h_d at four cut planes As illustrated in Fig. 5, a raise in h_d from 25.3 mm to 29.3 mm brings about a reduction in the HPBWs of the antenna at 1.207 GHz. The antenna shows the poor radiation characteristics at 1.561 GHz when h_d is 25.3 mm from Fig. 6. And when h_d increases from 26.3 mm to 29.3 mm, the HPBWs are decreased. Nevertheless, the value of h_d also affects the 3-dB ARBWs. When h_d increases, the ARBWs first increase and then decrease at two frequencies. In order to obtain wide ARBWs and HPBWs at 1.207 GHz and 1.561 GHz, the value of h_d is determined to be 27.3 mm.

Figures 7 and 8 illustrate the impact of h_j. The results show that HPBW increases with the increase of h_j at 1.207 GHz, and increases first and then decreases with the increase of h_j at 1.561 GHz. When h_j equals 29 mm and 31 mm, the radiation characteristics are almost the same. Because the length of h_j is longer than h_d, the metal columns will extend into substrate II. However, the value of h_j also affects the 3-dB ARBWs. The ARBWs increase first and then decrease with the increase of

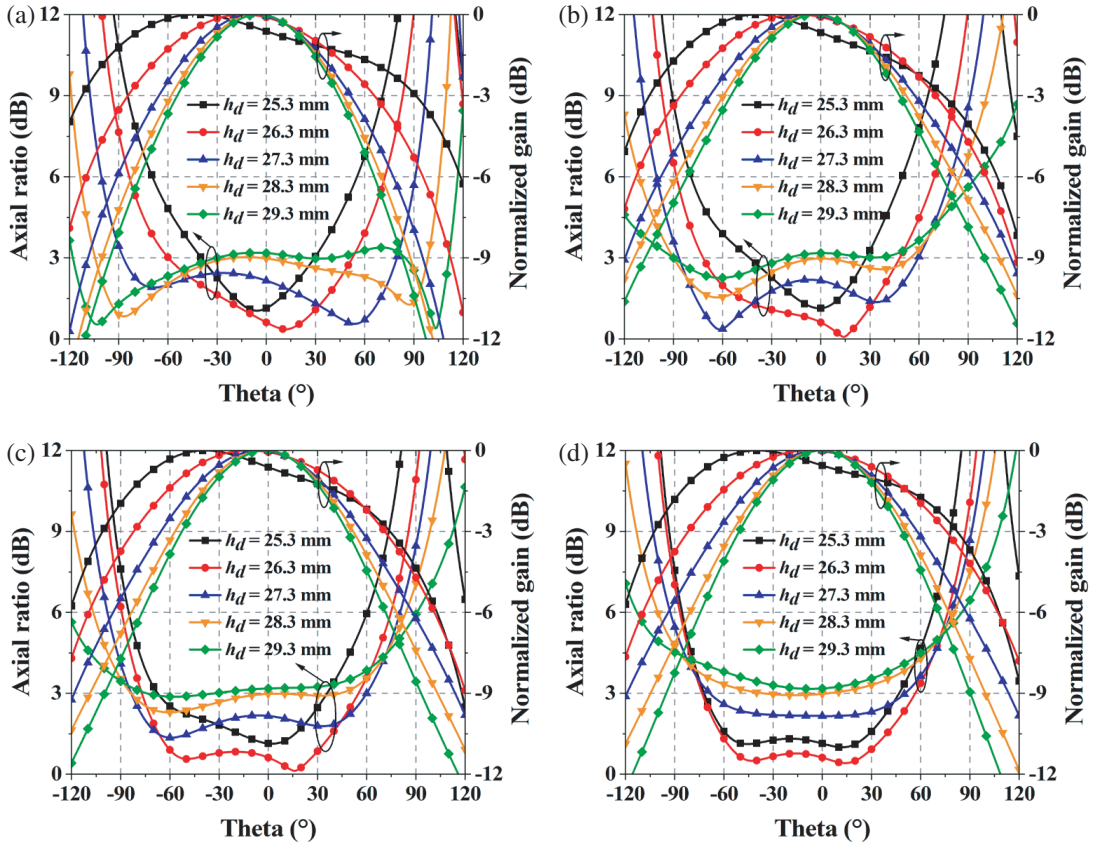

FIGURE 5. ARBWs and HPBWs for different h_d at 1.207 GHz (a) $\varphi = 0°$. (b) $\varphi = 45°$. (c) $\varphi = 90°$. (d) $\varphi = 135°$.

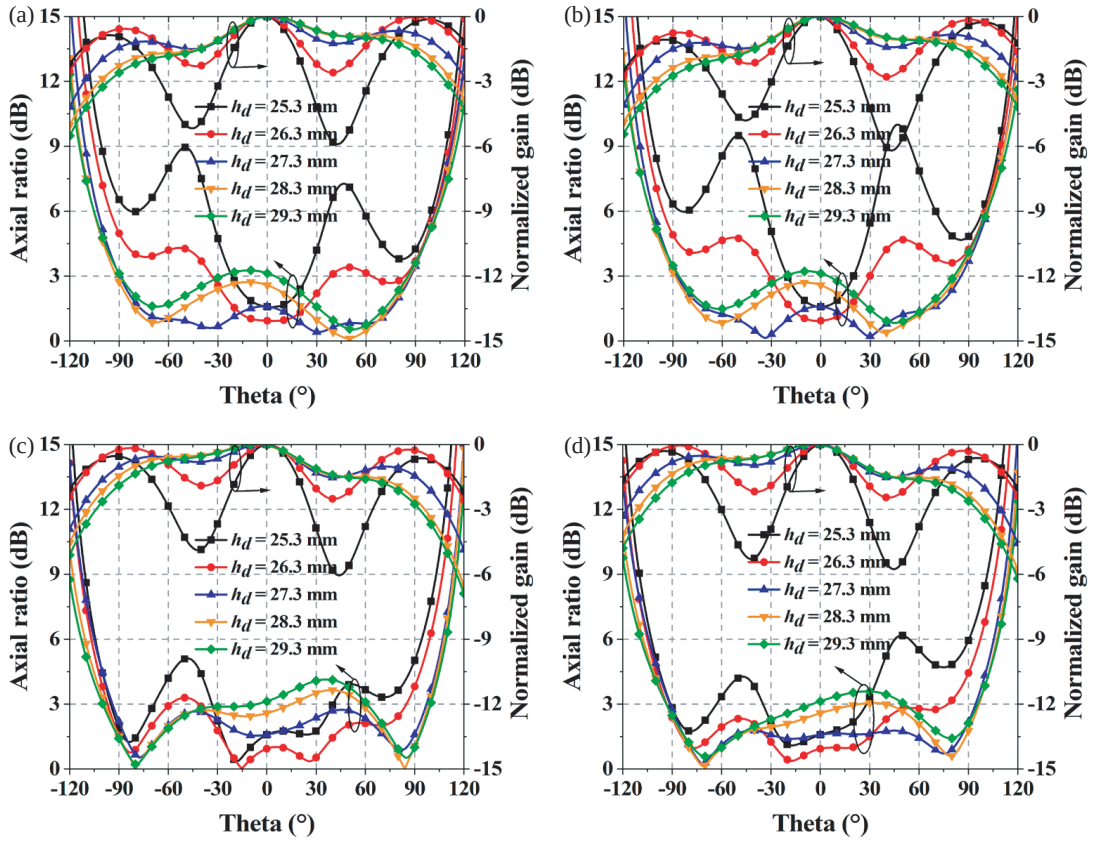

FIGURE 6. ARBWs and HPBWs for different h_d at 1.561 GHz (a) $\varphi = 0°$. (b) $\varphi = 45°$. (c) $\varphi = 90°$. (d) $\varphi = 135°$.

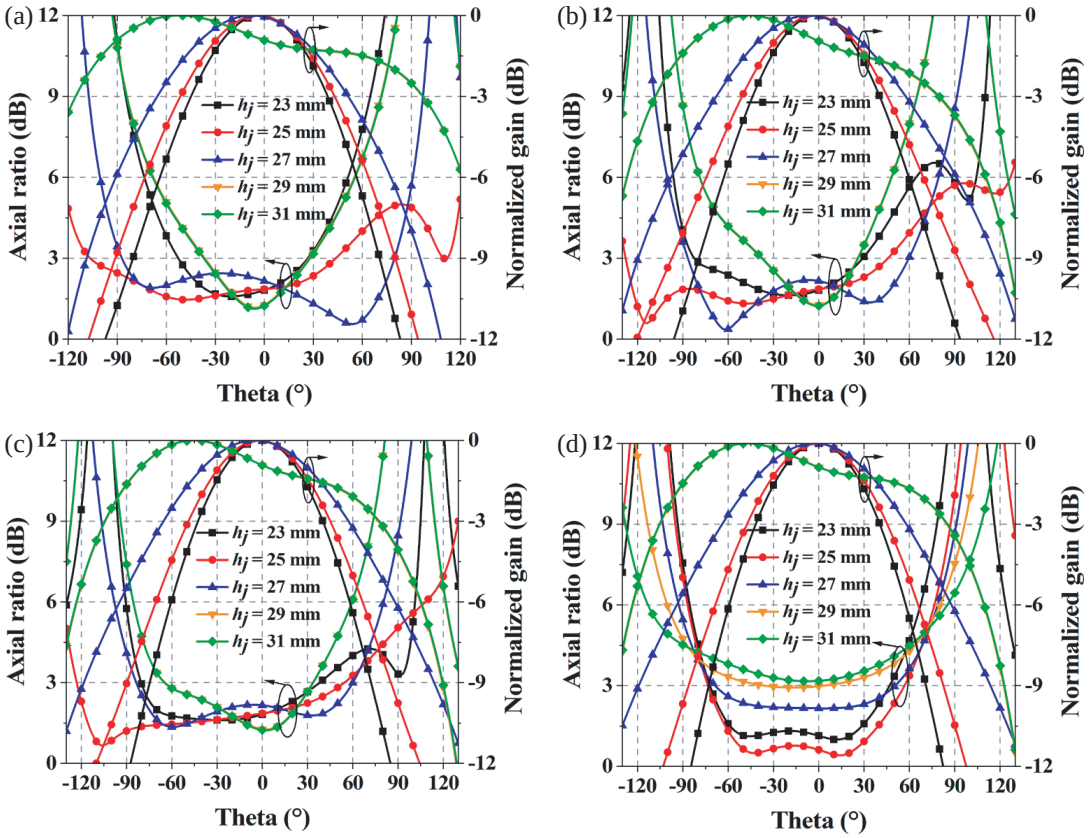

FIGURE 7. ARBWs and HPBWs for different h_j at 1.207 GHz (a) $\varphi = 0°$. (b) $\varphi = 45°$. (c) $\varphi = 90°$. (d) $\varphi = 135°$.

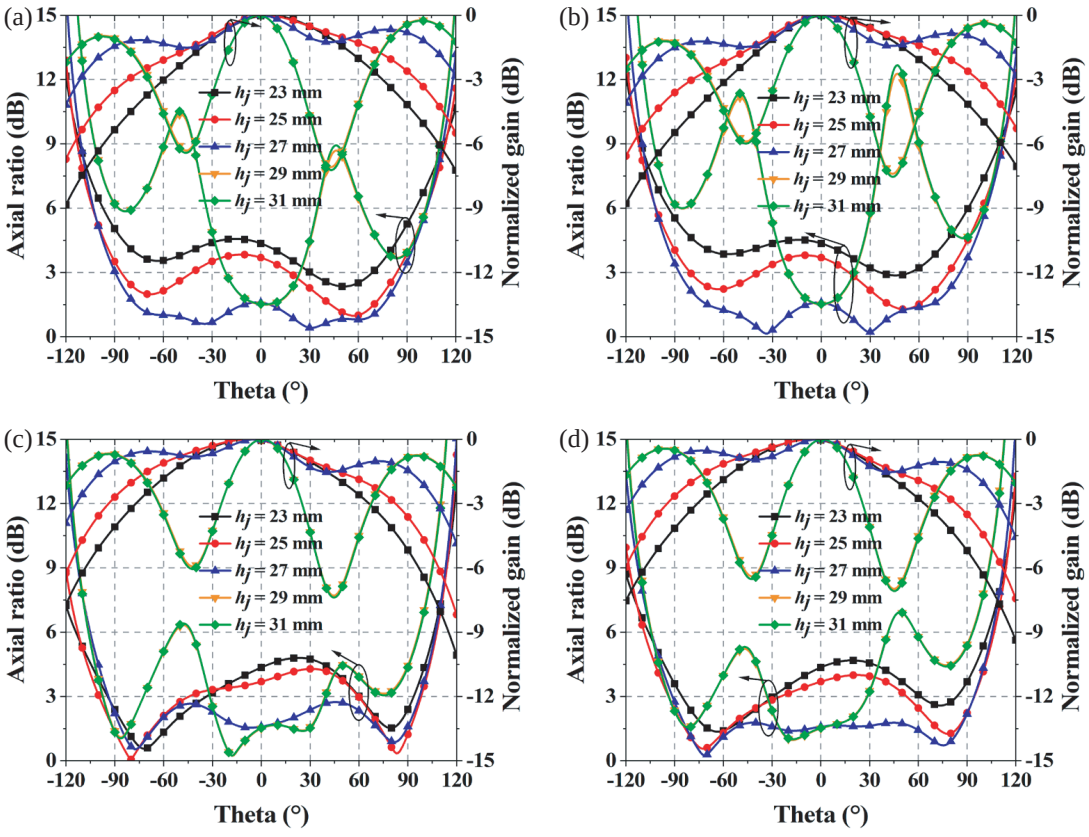

FIGURE 8. ARBWs and HPBWs for different h_j at 1.561 GHz (a) $\varphi = 0°$. (b) $\varphi = 45°$. (c) $\varphi = 90°$. (d) $\varphi = 135°$.

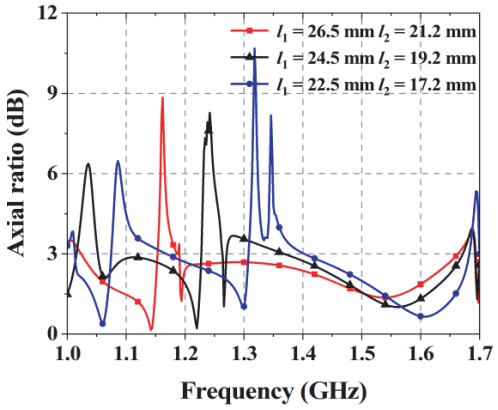

FIGURE 9. AR for different arm length of the dipole.

(a)

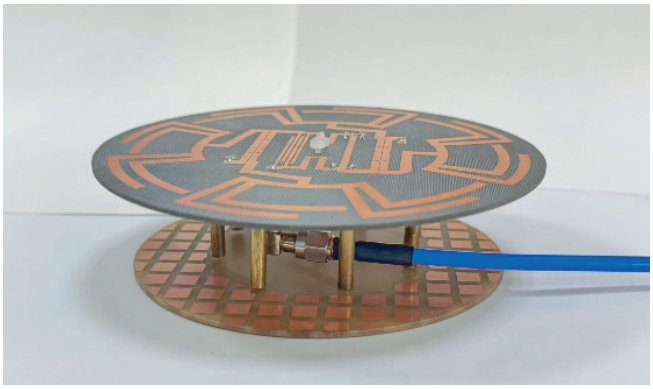

(b)

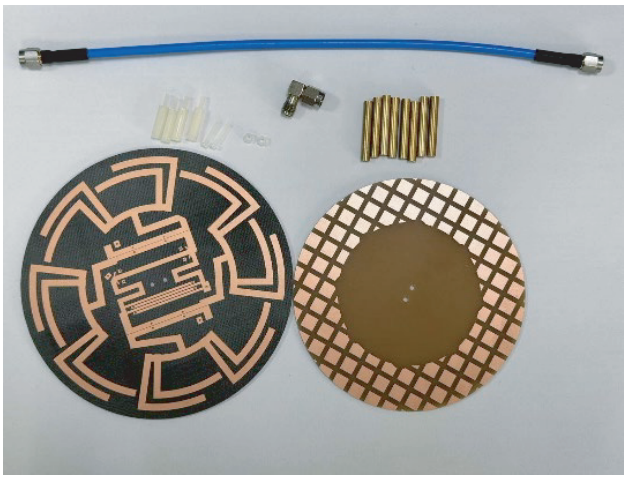

FIGURE 10. Picture of the fabricated CP antenna. (a) 3D view. (b) components.

h_j. To attain equilibrium, it is necessary to make a compromise. Finally, h_j is chosen to 27 mm

In addition, the relation between the arm length and AR performance is also investigated. Fig. 9 gives the AR of the antenna with different arm lengths of the dipole. It is seen that as l_1 and l_2 increase, the AR of the two bands moves toward the lower frequency. This phenomenon is corresponding to the design theory that the resonant frequency of the dipole is decreased with the increase of the arm length.

4. FABRICATION AND EXPERIMENTAL RESULTS

The fabrication and illustrative depiction of the prototype can be found in Fig. 10. The overall size is 120 mm × 120 mm × 30.3 mm, which corresponds to $0.48\lambda \times 0.48\lambda \times 0.12\lambda$ (λ is the wavelength in vacuum at 1.207 GHz). Fig. 11 plots the simulated and measured $||S_{11}|$, Gain, and AR. It is observed that the measured 10-dB impedance bandwidth is 44.8% (1.9 GHz to 1.72 GHz), while the AR is below 3 dB from 1.17 GHz to 1.22 GHz (4.2%) and 1.39 GHz to 1.65 GHz (17.1%). Under the criterion of gain larger than 0 dBic, the measured gain bandwidth is within 1.12 GHz ∼ 1.22 GHz (8.5%) and 1.5 GHz ∼ 1.68 GHz (11.3%). At 1.207 GHz and 1.561 GHz, the gains are 1.89 dBic and 0.79 dBic, respectively.

Figures 12 and 13 present the measured and simulated radiation patterns at 1.207 GHz and 1.561 GHz. The measured outcomes are approximately consistent with the simulated results. Since the gain for right hand circular polarization (RHCP) is larger than that for left hand circular polarization (LHCP), the polarization is RHCP. Besides, symmetric radiation performances can be observed.

Figures 14 and 15 show the simulated and measured ARBWs and HPBWs. As illustrated in Fig. 14, the measured 3-dB ARBWs of 1.207 GHz are 129°, 128°, 123°, and 121° at the planes of $\varphi = 0°$, 45°, 90°, and 135°, respectively. The consequential HPBWs are 121°, 123°, 121°, and 122°, respectively. From Fig. 15, the measured 3-dB ARBWs of 1.561 GHz are 155°, 150°, 158°, and 165° at the planes of $\varphi = 0°$, 45°, 90°, and 135°, respectively. And the consequential HPBWs are 208°, 202°, 198°, and 215°, respectively.

Table 1 illustrates the contrast between the previous studies and the proposed antenna. Although the works in [23] and [25] demonstrate a greater HPBW, these devices are constrained to single-band functionality, and the size is large. Compared with the dual-band CP antennas in [7, 19], the proposed antenna has a

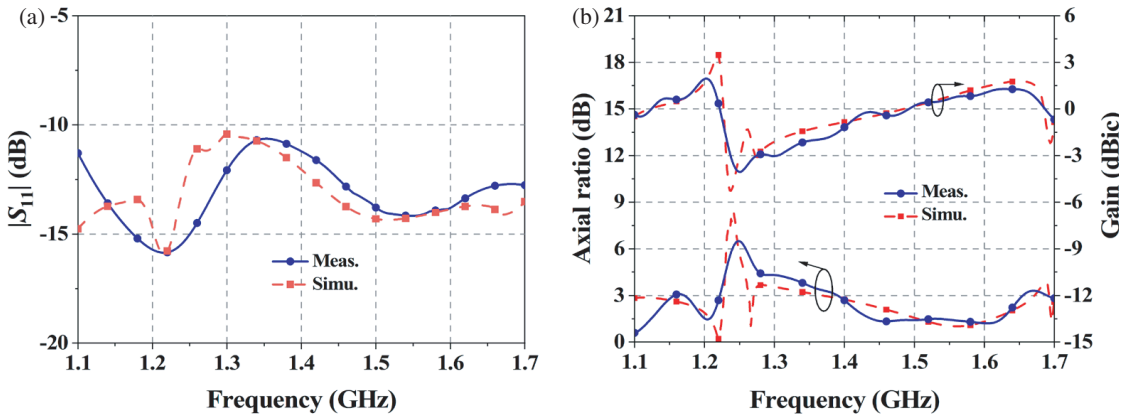

FIGURE 11. Measured and simulated results of the fabricated antenna. (a) $|S_{11}|$. (b) AR and gain.

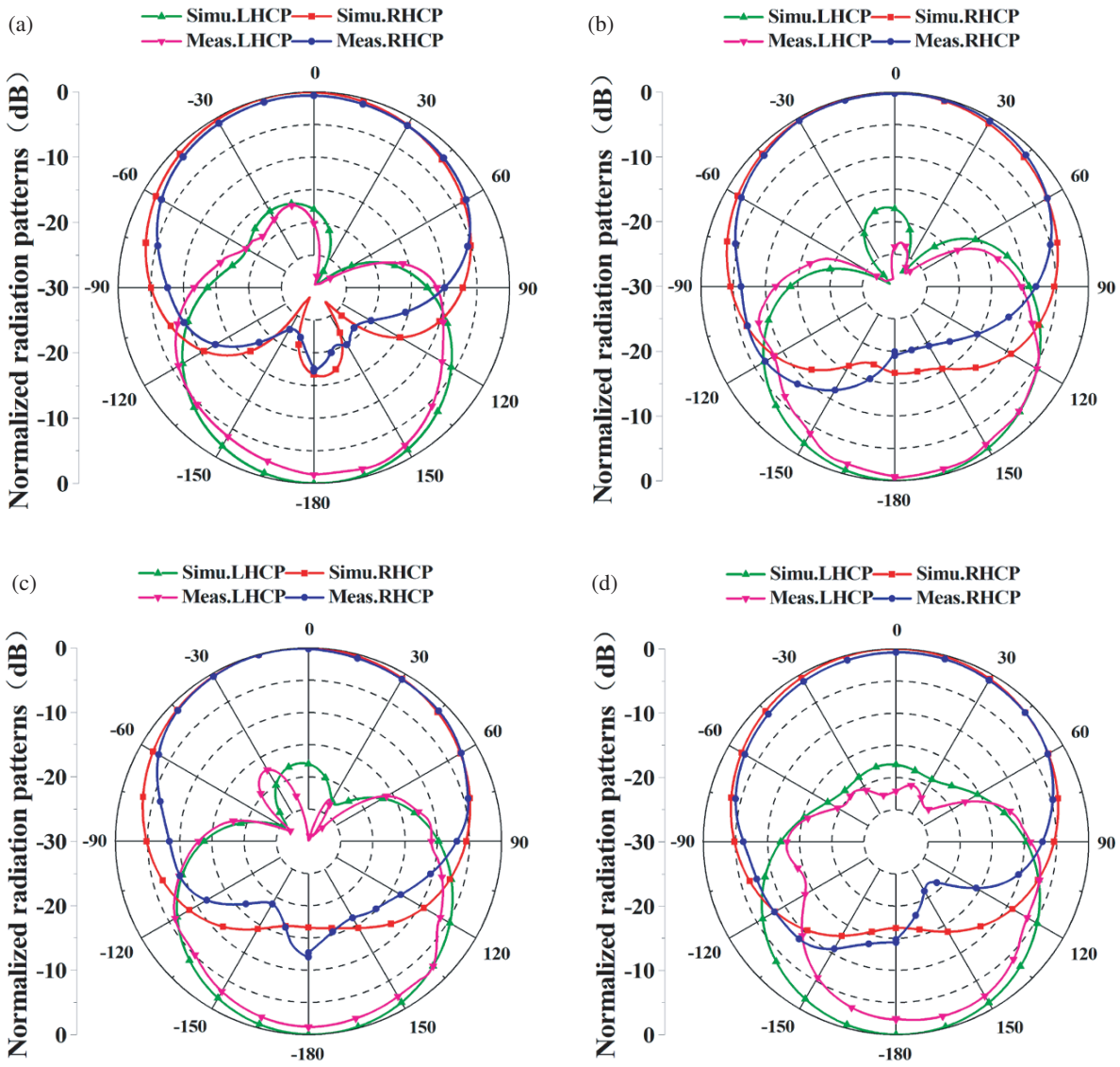

FIGURE 12. Measured and simulated radiation patterns of the proposed antenna at 1.207 GHz. (a) $\varphi = 0°$. (b) $\varphi = 45°$. (c) $\varphi = 90°$. (d) $\varphi = 135°$.

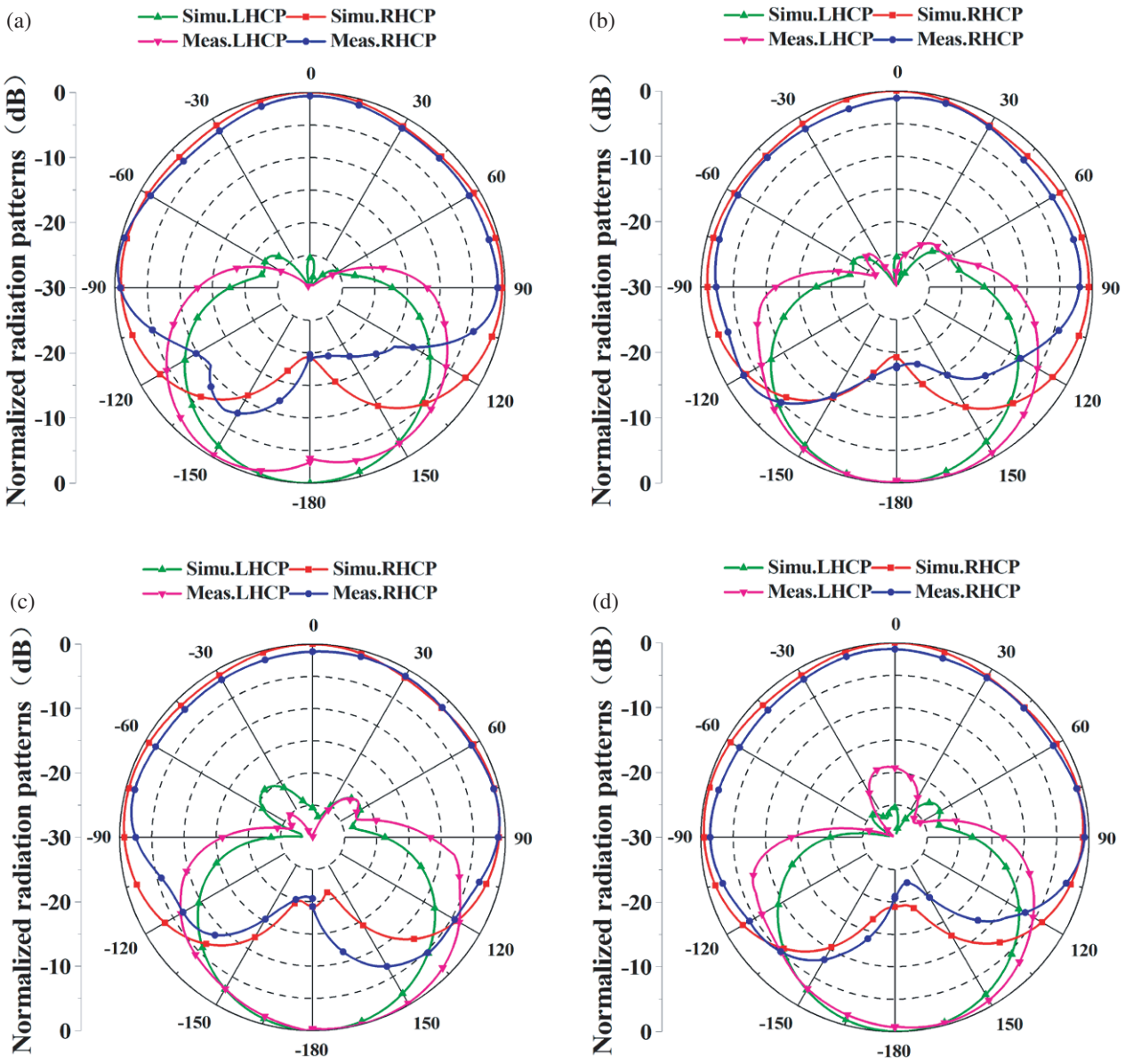

FIGURE 13. Measured and simulated radiation patterns of the proposed antenna at 1.561 GHz. (a) $\varphi = 0°$. (b) $\varphi = 45°$. (c) $\varphi = 90°$. (d) $\varphi = 135°$.

TABLE 1. Performance comparison between this work and previously reported wide-beam CP antennas.

Ref.	Frequency (GHz)	Overlapped bandwidth[a]	3-dB ARBW	HPBW	Overlapped beamwidth[b]	Size ($\lambda \times \lambda \times \lambda$)
[7]	1.227/1.575	13.0%/29.1%	202° /211°	103° /111°	103° /111°	0.7 × 0.7 × 0.58
[19]	1.268/1.602	55.8%	134° /196°	113° /111°	113° /111°	0.52 × 0.52 × 0.15
[21]	1.227/1.575	12.2%/5.1%	186° /163°	126° /120°	126° /120°	0.24 × 0.24 × 0.07
[23]	1.6	15.6%	203°	170°	170°	1.28 × 1.28 × 0.19
[25]	1.561	5.2%	142°	131°	131°	0.74 × 0.74 × 0.2
This work	1.207/1.561	4.2%/17.1%	121° /150°	121° /198°	121° /150°	0.48 × 0.48 × 0.12

[a] $|S_{11}| < -10$ dB & AR < 3 dB
[b] 3-dB ARBW & HPBW

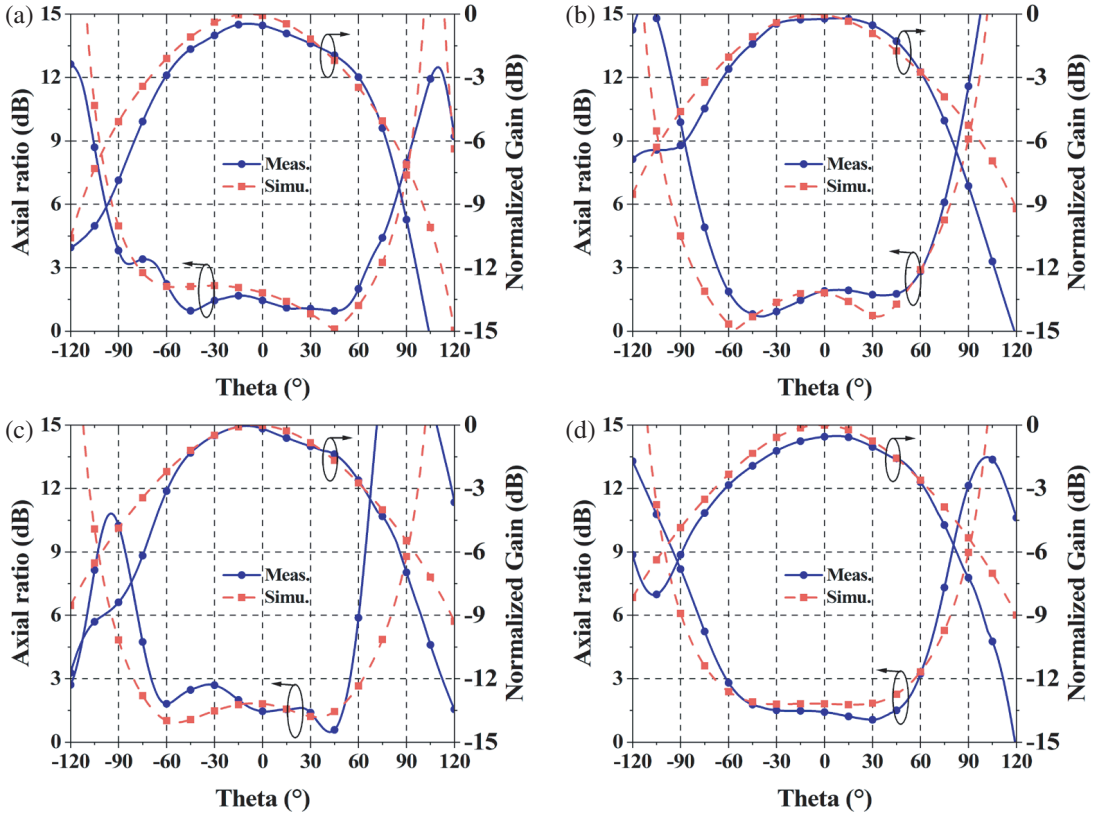

FIGURE 14. Measured and simulated ARBWs and HPBWs of the fabricated antenna at 1.207 GHz. (a) $\varphi = 0°$. (b) $\varphi = 45°$. (c) $\varphi = 90°$. (d) $\varphi = 135°$.

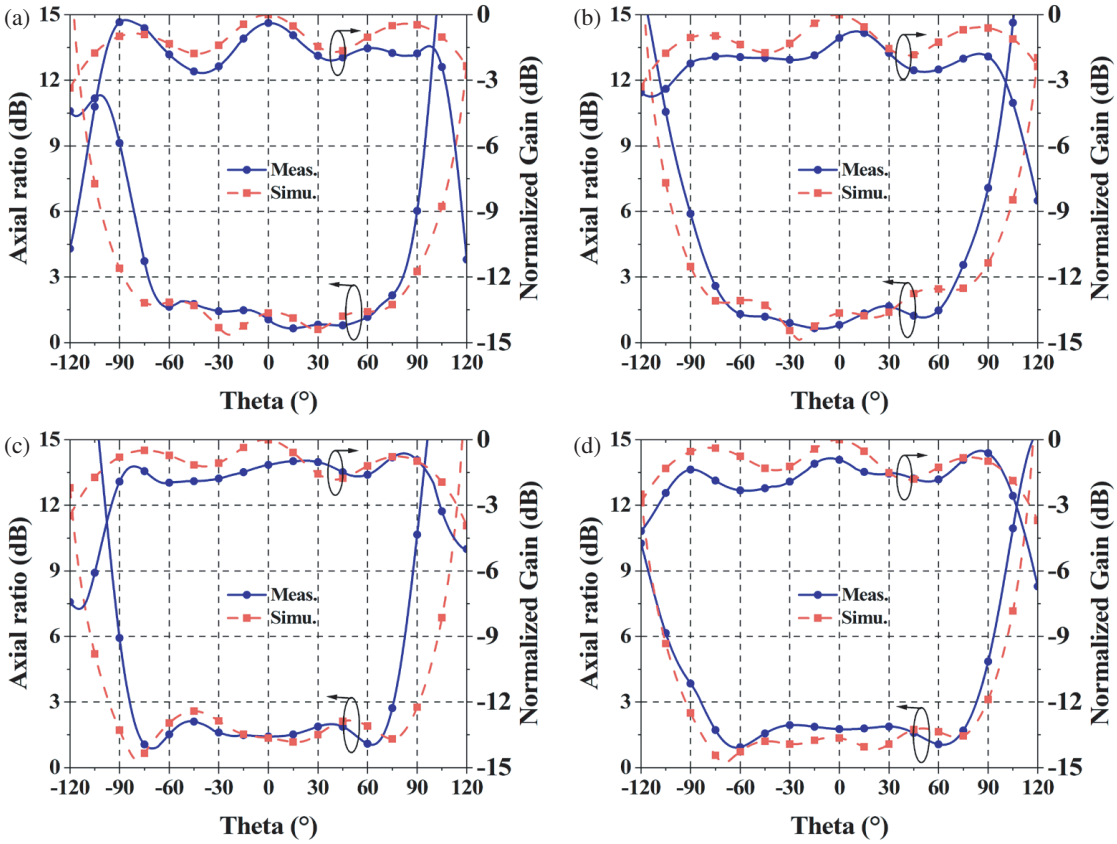

FIGURE 15. Measured and simulated ARBWs and HPBWs of the fabricated antenna at 1.561 GHz. (a) $\varphi = 0°$. (b) $\varphi = 45°$. (c) $\varphi = 90°$. (d) $\varphi = 135°$.

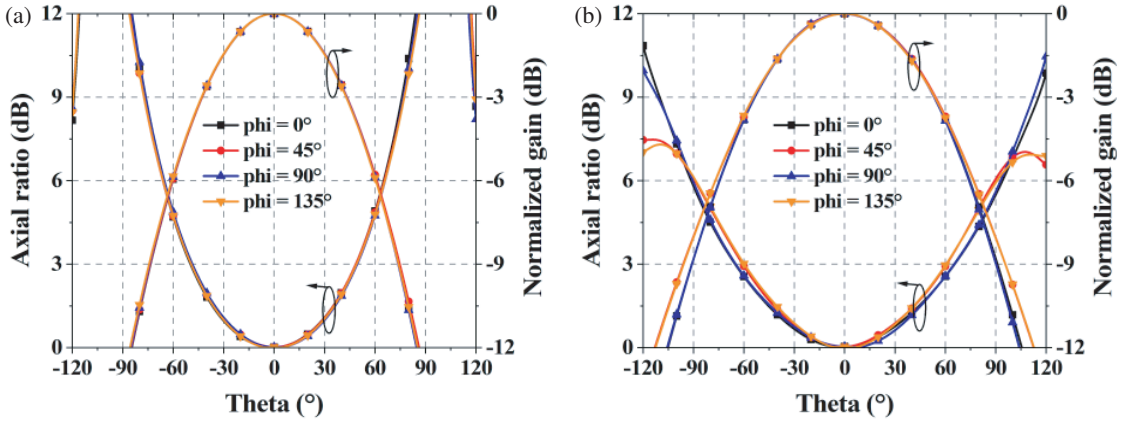

FIGURE 16. ARBWs and HPBWs of the antenna with metal plate (distance between the metal plate and the antenna is $\lambda/4$). (a) 1.207 GHz. (b) 1.561 GHz.

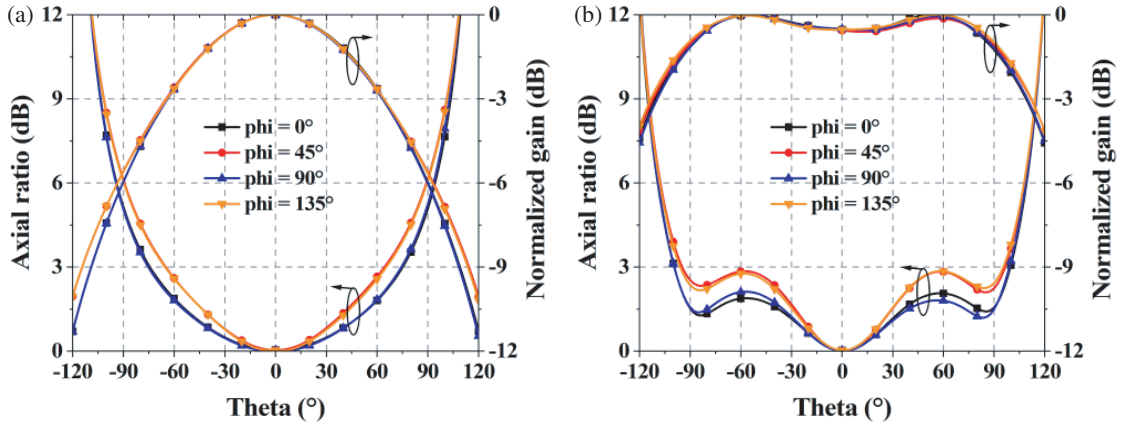

FIGURE 17. ARBWs and HPBWs of the antenna with RIS. (a) 1.207 GHz. (b) 1.561 GHz.

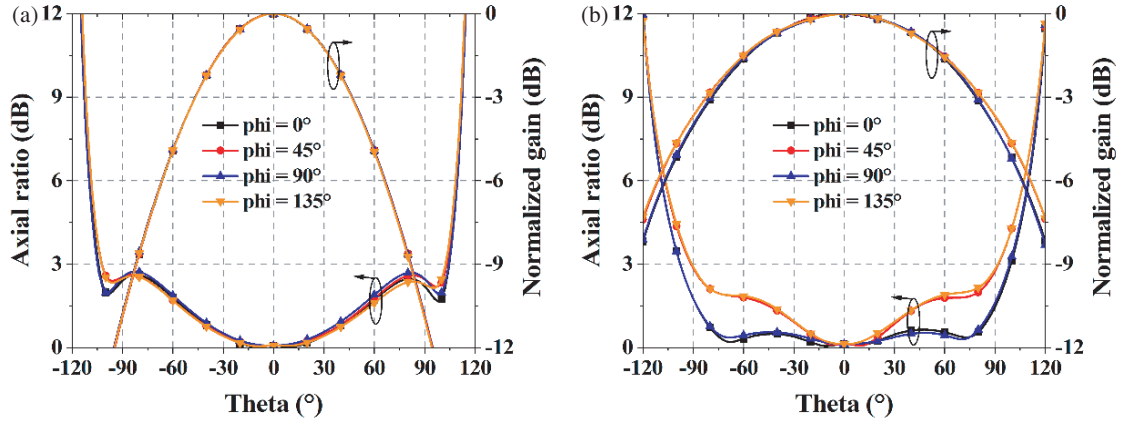

FIGURE 18. ARBWs and HPBWs of the antenna with the metal plate (same reflection phase as the RIS). (a) 1.207 GHz. (b) 1.561 GHz.

broader overlapped beamwidth. Also, the proposed antenna has a broader overlapped beamwidth at 1.561 GHz than the work in [21]. Furthermore, since all the referenced antennas focus on the beamwidths at two cut planes (xoz and yoz planes), there is a lack of certainty regarding the radiation characteristics. However, the proposed antenna is designed to consider radiation performance across four cut planes.

5. DISCUSSION

In this section, the differences between the RIS and the metal plate on the beamwidth improvement of the antenna are discussed. Here, two cases are investigated.

Case 1: the metal plate is used to replace the RIS, and the distance between the metal plate and the antenna is $\lambda/4$.

Figure 16 gives the ARBW and HPBW performances in case 1. It is observed that the HPBWs at 1.207 GHz and 1.561 GHz are 86° and 106°, respectively, while the 3-dB ARBWs are 98° and 120°/130° at 1.207 GHz and 1.561 GHz, respectively. Fig. 17 shows the ARBW and HPBW performances with RIS. It is seen that the HPBWs at 1.207 GHz and 1.561 GHz are 128° and 220°/224°, respectively. While the corresponding 3-dB ARBWs are 130°/148° and 192°/198°.

Comparing the metal plate in case 1 with the RIS, it is found that the RIS is benefit for the beamwidth enhancement at the dual bands. This is because the RIS is used not only for obtaining unidirectional radiation, but also for beamwidth improvement, while the metal plate with $\lambda/4$ distance only shows the function of unidirectional radiation.

Case 2: the metal plate is used to replace the RIS, and the distance between the metal plate and the antenna achieves the same reflection phase as the RIS.

Figure 18 gives the ARBW and HPBW performances in case 2. It is observed that the HPBWs at 1.207 GHz and 1.561 GHz are 92° and 160°/164°, respectively, while the 3-dB ARBWs are 204° and 184°/196° at 1.207 GHz and 1.561 GHz, respectively. Comparing the metal plate in case 2 with the RIS, it is found that although satisfying equal reflection phase, the RIS still shows better performance of HPBW. While in case 2, the 3-dB ARBW is improved obviously, but the HPBW at the lower frequencies is rarely changed. Finally, the RIS is demonstrated to be more suitable for both HPBW and ARBW enhancement of the circularly polarized antenna.

6. CONCLUSION

In this paper, a dual-band CP antenna with wide overlapped beamwidth is presented, which is based on the adoption of bending dipoles, metal columns and an RIS. The results of the measurement indicate that the presented antenna can cover BDS B1 and B2 bands. At 1.207 GHz and 1.561 GHz, the overlapped beamwidth larger than 121° and 150° is obtained. In summary, the proposed antenna exhibits several advantages, including a wide overlapped beamwidth, a wide AR bandwidth, and a relatively compact size, which attributes a promising candidate for BDS applications.

ACKNOWLEDGEMENT

This work was supported in part by the National Natural Science Foundation of China under Grant 51809030, in part by the Liaoning Revitalization Talents Program under Grant XLYC2007067, in part by the Young Elite Scientists Sponsorship Program by CAST under Grant 2022QNRC001 and in part by the Fundamental Research Funds for the Central Universities under Grant 3132024239.

REFERENCES

[1] Wang, S., X. Zhang, L. Zhu, and W. Wu, "Single-fed wide-beamwidth circularly polarized patch antenna using dual-function 3-D printed substrate," *IEEE Antennas and Wireless Propagation Letters*, Vol. 17, No. 4, 649–653, 2018.

[2] Ferrero, F., C. Luxey, G. Jacquemod, and R. Staraj, "Dual-band circularly polarized microstrip antenna for satellite applications," *IEEE Antennas and Wireless Propagation Letters*, Vol. 4, 13–15, 2005.

[3] Pozar, D. M. and S. M. Duffy, "A dual-band circularly polarized aperture-coupled stacked microstrip antenna for global positioning satellite," *IEEE Transactions on Antennas and Propagation*, Vol. 45, No. 11, 1618–1625, 1997.

[4] Liu, Q., Y. Liu, Y. Wu, M. Su, and J. Shen, "Compact wideband circularly polarized patch antenna for CNSS applications," *IEEE Antennas and Wireless Propagation Letters*, Vol. 12, 1280–1283, 2013.

[5] Zheng, K.-K. and Q.-X. Chu, "A novel annular slotted center-fed BeiDou antenna with a stable phase center," *IEEE Antennas and Wireless Propagation Letters*, Vol. 17, No. 3, 364–367, 2018.

[6] Liu, S., D. Yang, and J. Pan, "A low-profile circularly polarized metasurface antenna with wide axial-ratio beamwidth," *IEEE Antennas and Wireless Propagation Letters*, Vol. 18, No. 7, 1438–1442, 2019.

[7] Sun, Y.-X., K. W. Leung, and J. Ren, "Dual-band circularly polarized antenna with wide axial ratio beamwidths for upper hemispherical coverage," *IEEE Access*, Vol. 6, 58 132–58 138, 2018.

[8] Zheng, D.-Z., Y. Luo, and Q.-X. Chu, "Cavity-backed self-phased circularly polarized multidipole antenna with wide axial-ratio beamwidth," *IEEE Antennas and Wireless Propagation Letters*, Vol. 16, 1998–2001, 2017.

[9] Chen, R.-S., L. Zhu, S.-W. Wong, J.-Y. Lin, Y. Li, L. Zhang, and Y. He, "S-band full-metal circularly polarized cavity-backed slot antenna with wide bandwidth and wide beamwidth," *IEEE Transactions on Antennas and Propagation*, Vol. 69, No. 9, 5963–5968, 2021.

[10] Luo, Y., Q.-X. Chu, and L. Zhu, "A miniaturized wide-beamwidth circularly polarized planar antenna via two pairs of folded dipoles in a square contour," *IEEE Transactions on Antennas and Propagation*, Vol. 63, No. 8, 3753–3759, 2015.

[11] Zhang, X., L. Zhu, and N.-W. Liu, "Pin-loaded circularly-polarized patch antennas with wide 3-dB axial ratio beamwidth," *IEEE Transactions on Antennas and Propagation*, Vol. 65, No. 2, 521–528, 2017.

[12] Wang, M.-S., X.-Q. Zhu, Y.-X. Guo, and W. Wu, "Compact circularly polarized patch antenna with wide axial-ratio beamwidth," *IEEE Antennas and Wireless Propagation Letters*, Vol. 17, No. 4, 714–718, 2018.

[13] Ray, M. K., K. Mandal, and N. Nasimuddin, "Low-profile circularly polarized patch antenna with wide 3 dB beamwidth," *IEEE Antennas and Wireless Propagation Letters*, Vol. 18, No. 12, 2473–2477, 2019.

[14] Liu, H., Y. Zhang, Y. Wang, S. Fang, and Z. Wang, "Circular polarized patch antenna with wide 3-dB axial ratio beamwidth and suppressed backward cross-polarized radiation for high-precision marine navigation applications," *IET Microwaves, Antennas & Propagation*, Vol. 15, No. 11, 1393–1401, 2021.

[15] Li, G. and F.-S. Zhang, "A compact broadband and wide beam circularly polarized antenna with shorted vertical plates," *IEEE Access*, Vol. 7, 90 916–90 921, 2019.

[16] Feng, B., L. Li, K. L. Chung, and Y. Li, "Wideband widebeam dual circularly polarized magnetoelectric dipole antenna/array with meta-columns loading for 5G and beyond," *IEEE Transactions on Antennas and Propagation*, Vol. 69, No. 1, 219–228, 2021.

[17] Wang, L., Z. Weng, Y.-C. Jiao, W. Zhang, and C. Zhang, "A low-profile broadband circularly polarized microstrip antenna with wide beamwidth," *IEEE Antennas and Wireless Propaga-*

tion Letters, Vol. 17, No. 7, 1213–1217, 2018.

[18] Wang, Z., S. Liu, and Y. Dong, "Electrically small, low-Q, wide beam-width, circularly polarized, hybrid magnetic dipole antenna for RFID application," *IEEE Transactions on Antennas and Propagation*, Vol. 69, No. 10, 6284–6293, 2021.

[19] Yan, Y.-D., Y.-C. Jiao, C. Zhang, Y.-X. Zhang, and G.-T. Chen, "Hemispheric conformal wide beamwidth circularly polarized antenna based on two pairs of curved orthogonal dipoles in space," *IEEE Transactions on Antennas and Propagation*, Vol. 69, No. 11, 7900–7905, 2021.

[20] Yang, W. J., Y. M. Pan, and S. Y. Zheng, "A low-profile wideband circularly polarized crossed-dipole antenna with wide axial-ratio and gain beamwidths," *IEEE Transactions on Antennas and Propagation*, Vol. 66, No. 7, 3346–3353, 2018.

[21] Liu, H., M. Shi, S. Fang, and Z. Wang, "Design of low-profile dual-band printed quadrifilar helix antenna with wide beamwidth for UAV GPS applications," *IEEE Access*, Vol. 8, 157 541–157 548, 2020.

[22] Luo, Y., X. Wang, and L. Zhu, "Beamwidth-enhanced circularly polarized antenna using non-uniformly compressed high-order mode dipoles," *IEEE Transactions on Antennas and Propagation*, Vol. 70, No. 9, 7831–7842, 2022.

[23] Liu, H., C. Mu, T. Yan, S. Fang, G. Wang, and Z. Wang, "Dielectric lens with stacked cone-shaped cavity for broadside radiation enhancement of circularly polarised patch antenna," *IET Microwaves, Antennas & Propagation*, Vol. 14, No. 13, 1610–1618, 2020.

[24] Yuan, Y., M. Wang, Y. Yin, and W. Wu, "Wide-beam circularly polarized microstrip antenna with high front-to-back ratio for CNSS application," in *2017 Sixth Asia-Pacific Conference on Antennas and Propagation (APCAP)*, 1–3, Xi'an, China, 2017.

[25] Ren, J., H. Liu, D. Yu, Y. Zeng, and Z. Wang, "Design of circularly polarized antenna with wide overlapped axial-ratio and gain beamwidths for upper hemispherical coverage," *Microwave and Optical Technology Letters*, Vol. 66, No. 2, e34038, 2024.

[26] Zheng, Y., W. Wang, Y. Yang, and Y. Wu, "Single-layer planar wideband rat-race coupler using a shorted parallel-coupled multi-line section," *IEEE Transactions on Circuits and Systems II: Express Briefs*, Vol. 67, No. 12, 3053–3057, 2020.

[27] Liang, C.-H., W.-S. Chang, and C.-Y. Chang, "Enhanced coupling structures for tight couplers and wideband filters," *IEEE Transactions on Microwave Theory and Techniques*, Vol. 59, No. 3, 574–583, 2011.